BIOCHEMISTRY
including biophysical chemistry & molecular biology

Article

pubs.acs.org/biochemistry

Crucial Effects of Amino Acid Side Chain Length in Transmembrane Segment 5 on Substrate Affinity in Yeast Glucose Transporter Hxt7

Toshiko Kasahara,*[,†] Kosuke Shimogawara,[‡] and Michihiro Kasahara[†,§]

[†]Laboratory of Biophysics, School of Medicine, [‡]Laboratory of Chemistry, School of Medicine, and [§]Genome Research Center, Teikyo University, Hachioji, Tokyo 192-0395, Japan

Supporting Information

ABSTRACT: We previously identified Asp[340] in transmembrane segment 7 (TM7) as a key determinant of substrate affinity in Hxt7, a high-affinity facilitative glucose transporter of *Saccharomyces cerevisiae*. To gain further insight into the structural basis of substrate recognition by Hxt7, we performed cysteine-scanning mutagenesis of 21 residues in TM5 of a Cys-less form of Hxt7. Four residues were sensitive to Cys replacement, among which Gln[209] was found to be essential for high-affinity glucose transport activity. The 17 remaining sites were examined further for the accessibility of cysteine to the hydrophilic sulfhydryl reagent *p*-chloromercuribenzenesulfonate (pCMBS). Among the Cys mutants, T213C was the only one whose transport activity was completely inhibited by 0.5 mM pCMBS. Moreover, this mutant was protected from pCMBS inhibition by the substrate D-glucose and by 2-deoxy-D-glucose but not by L-glucose, indicating that Thr[213] is situated at or close to a substrate recognition site. The functional role of Thr[213] was further examined with its replacement with each of the other 19 amino acids in wild-type Hxt7. Such replacement generated seven functional transporters with various affinities for glucose. Only three mutants, those with Val, Cys, and Ser at position 213, exhibited high-affinity glucose transport activity. All of these residues possess a side chain length similar to that of Thr, indicating that side chain length at this position is a key determinant of substrate affinity. A working homology model of Hxt7 indicated that Gln[209] and Thr[213] face the central cavity and that Thr[213] is located within van der Waals distance of Asp[340] (TM7).

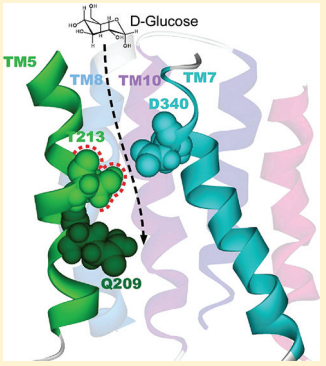

The preferred carbon sources for most prokaryotic and eukaryotic cells are carbohydrates, above all the monosaccharide glucose. The obligate first step of sugar metabolism is sugar transport. In the yeast *Saccharomyces cerevisiae*, hexoses are made available for cellular metabolism by facilitated diffusion across the plasma membrane mediated by a wide variety of transporters, including Hxt1−Hxt11, Hxt13−Hxt17, and Gal2.[1,2] All of these transporters belong to the major facilitator superfamily (MFS),[3] and they contain 12 putative transmembrane segments (TMs) as well as intracellular NH_2 and COOH termini. The MFS includes a variety of transporters for organic solutes in prokaryotes, archaea, and eukaryotes. Elucidation of the three-dimensional (3D) structures of five bacterial MFS transporters, including an oxalate transporter (OxlT) of *Oxalobacter formigenes*[4] as well as a lactose permease (LacY),[5] glycerol-3-phosphate transporter (GlpT),[6] multidrug transporter (EmrD),[7] and L-fucose transporter (FucP)[8] of *Escherichia coli*, has led to the notion that all MFS transporters share a similar topological organization of TMs with a centrally located hydrophilic substrate translocation pathway.

We have previously studied which residues of glucose transporter Hxt2 are important for its moderately high substrate affinity (K_m = 3.3 mM) by generating a comprehensive series of chimeric transporters between Hxt2 and Hxt1, a low-affinity glucose transporter (K_m = 46 mM).[9,10] We found that Asn[331] in TM7 is a key residue responsible for the moderately high-affinity glucose transport activity of Hxt2.[11] We also examined the possible existence of a common structure around this residue in yeast hexose transporters with the use of Hxt7, a high-affinity glucose transporter (K_m = 0.72 mM). We identified Asp[340] of Hxt7, which corresponds to Asn[331] of Hxt2, as a key residue that determines glucose affinity in Hxt7, suggesting that the mechanism of substrate recognition is similar in Hxt7 and Hxt2. We also found that Asp[340] is located at or close to a substrate recognition site in Hxt7 by application of the substituted cysteine accessibility method (SCAM) to TM7 and with the use of a substrate protection assay.[12]

To gain further insight into the structural basis of substrate recognition by Hxt7, we have now investigated the role of TM5, which, together with TM7, -8, and -10, contributes to the wall surrounding the substrate pathway in the crystal structures of bacterial MFS transporters.[4−8] We performed cysteine-scanning analysis of TM5 in a functional Cys-less form of Hxt7 in conjunction with exposure to the hydrophilic sulfhydryl reagent *p*-chloromercuribenzenesulfonate (pCMBS) to allocate residues of TM5 to the substrate translocation pathway. With this approach, we found that Gln[209] is an essential residue for the high-affinity glucose transport activity of Hxt7 and that Thr[213] is situated at or close to the substrate recognition site. We further investigated the role of Thr[213] in wild-type Hxt7 by

Received: July 5, 2011
Revised: September 2, 2011
Published: September 5, 2011

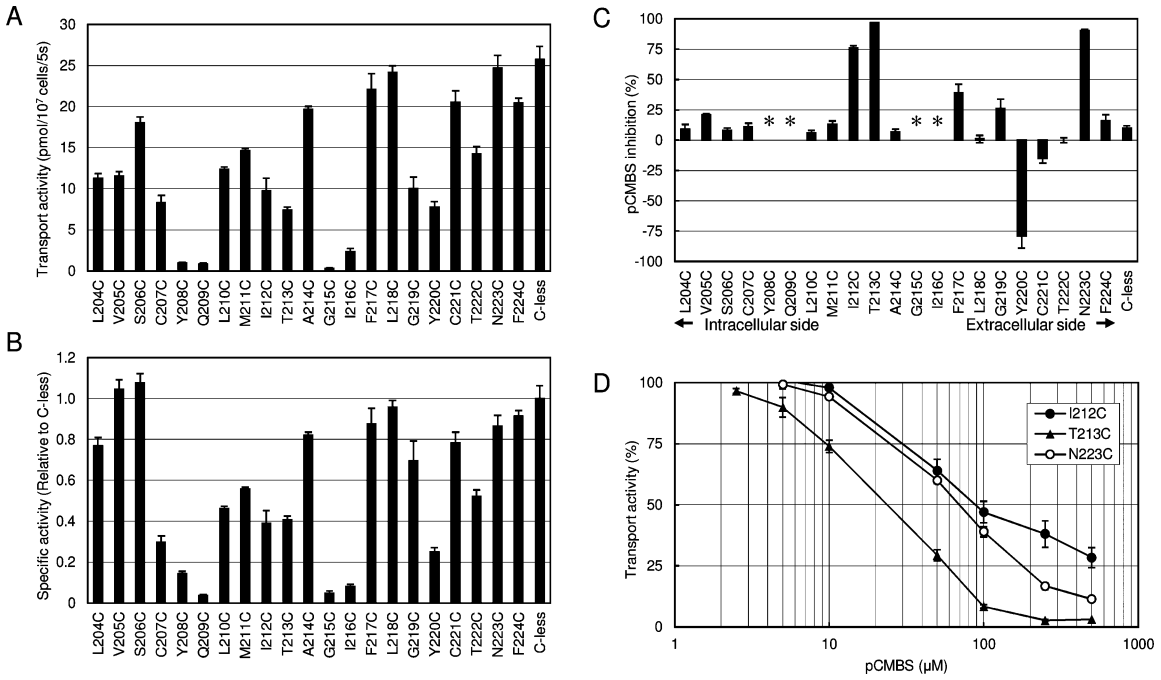

Figure 1. Glucose transport activities of single-Cys mutants of Hxt7 and effects of pCMBS. (A and B) Each residue in TM5 of Cys-less Hxt7 (C-less) was individually replaced with cysteine to yield 21 mutants (L204C to F224C). KY73 cells harboring plasmids encoding each mutant were grown to log phase at 30 °C in SMal(ura) medium, after which glucose transport activity was measured for 5 s at 30 °C with 0.1 mM D-glucose as the substrate. Transport activity was normalized by cell number (A), or it was normalized by the expression level of each mutant as determined by quantitative immunoblot analysis (Figure S2 of the Supporting Information) and then expressed relative to the value for Cys-less Hxt7 (B). Data are means ± SE (n = 3). (C) KY73 cells expressing individual single-Cys mutants were incubated in the absence or presence of 0.5 mM pCMBS for 15 min at 30 °C before measurement of transport activity with 0.1 mM D-glucose as the substrate. Data are expressed as the percent inhibition of transport activity by pCMBS and are means ± SE (n = 4). Asterisks denote mutants for which pCMBS inhibition was not assessed because of their low glucose transport activities. (D) Cells expressing the I212C, T213C, or N223C mutant were incubated with the indicated concentration of pCMBS for 15 min at 30 °C before measurement of transport activity with 0.1 mM D-glucose as the substrate. Glucose transport activities are expressed as a percentage of that determined without pCMBS and are means ± SE ($n \geq 3$).

replacing it with each of the other 19 amino acid residues and thereby found that the side chain length of Thr^{213} is a key determinant of substrate affinity.

EXPERIMENTAL PROCEDURES

Vector Construction. We constructed plasmid Hxt7mnx-pVT to confer expression of *HXT7* under the control of the *ADH1* promoter in the multicopy plasmid pVT102-U (*YEp URA3 bla*).[12] Hxt7mnx-pVT was introduced into *S. cerevisiae* strain KY73 (*MATα hxt1Δ::HIS3::Δhxt4 hxt5::LEU2 hxt2Δ::HIS3 hxt3Δ::LEU2::Δhxt6 hxt7Δ::HIS3 gal2Δ::DR ura3−52 MAL2 SUC2 MEL*).[13]

Cysteine-Scanning Analysis. Replacement of all 11 cysteine residues of Hxt7 with Ala, with the exception of Cys^{389}, which was replaced with Thr, yielded a functional Cys-less Hxt7 mutant, as we previously described.[12] With the use of polymerase chain reaction-based site-directed mutagenesis, we changed each of the 21 residues in TM5 of Cys-less Hxt7 individually to cysteine. The amplification products were digested with restriction enzymes and substituted for the corresponding region of Cys-less *HXT7* in Hxt7mnx-pVT. The resulting plasmids were introduced into *S. cerevisiae* KY73 to yield 21 single-Cys mutants of TM5. The DNA sequence for each of the mutated transporters was confirmed with a DNA sequencer (model 310, Applied Biosystems).

Mutagenesis. Replacement of Tyr^{208}, Gln^{209}, or Thr^{213} in wild-type Hxt7 with each of the other 19 amino acid residues was performed with the use of a polymerase chain reaction-based approach in which the target codon, UAC (Tyr^{208}), CAA (Gln^{209}), or ACU (Thr^{213}), was replaced with a specific codon for each of the other 19 residues to generate mutant Y208X, Q209X, or T213X, respectively, as described previously.[14]

Transport Assay. Cells harboring plasmids were grown to log phase (optical density at 650 nm of 0.3−0.6) at 30 °C in a synthetic liquid medium containing 2% maltose supplemented with adenine and amino acids but not with uracil [SMal-(ura)].[15] Transport of glucose by the cells was measured at 30 °C for 5 s in a transport assay medium containing 50 mM MES-NaOH (pH 6.0) and 2 mM $MgSO_4$, as previously described.[16,17] Transport activities measured at a D-[^{14}C]-glucose concentration of 0.1 or 20 mM were expressed as picomoles of glucose per 1 × 10^7 cells per 5 s and were corrected for the background activity determined either in the presence of 0.5 mM $HgCl_2$ or with 0.1 or 20 mM L-[^{14}C]glucose as the substrate. Kinetic parameters were measured under the zero-trans entry condition and were determined by nonlinear regression analysis. For examination of the effects of pCMBS, cells were exposed to the agent for 15 min at 30 °C before the measurement of transport activity.

Construction of a 3D Model of Hxt7. A working homology model of Hxt7 was constructed with the use of the 3D structure alignment tool MODELER in the protein modeling package Discovery Studio (Accelrys) with the crystal structure of GlpT (Protein Data Bank entry 1PW4) as a reference structure and sequence alignment of GlpT and Hxt7 performed in house as described previously[10] with a slight

modification by referring structural features suggested by TMHMM (http://www.cbs.dtu.dk/services/TMHMM) and SOSUI (http://bp.nuap.nagoya-u.ac.jp/sosui). The initial model structure was energetically optimized with the use of the CHARMm forcefield and an energy minimization algorithm in the modeling package as described above.

Other Assays. A crude membrane fraction was prepared from cells as described previously[18] and was subjected to immunoblot analysis with rabbit polyclonal antibodies generated in response to a peptide comprising the 13 COOH-terminal residues of Hxt7 coupled to keyhole limpet hemocyanin. Immune complexes were detected with ^{125}I-labeled protein A (GE Healthcare or Perkin-Elmer) and were quantitated with the use of imaging plates (BAS 1800II, Fuji Film)[18] within the intensity range proportional to the amount of protein. The cell number was determined with a particle counter (Z2, Beckman Coulter) after exposure of cultures to ultrasonic treatment (Sonifier 450 equipped with a cup horn, Branson) for 15 s to disperse aggregated cells. The protein concentration was measured with bicinchoninic acid (Pierce).

RESULTS AND DISCUSSION

Cysteine-Scanning Analysis of TM5. We generated a series of 21 mutants (L204C to F224C) of TM5 of Cys-less Hxt7 by separately changing each residue to cysteine. The resulting mutant proteins were expressed in KY73 cells, in which genes for the eight major glucose transporters (Hxt1–Hxt7 and Gal2) were disrupted and therefore did not exhibit substantial glucose transport activity. Expression of each mutant protein was confirmed by immunoblot analysis of a crude membrane fraction with antibodies to Hxt7 (Figure S1A of the Supporting Information). All the transformed cells yielded a predominant immunoreactive band of ~49 kDa, corresponding to the position of Cys-less Hxt7. The expression levels of the single-Cys mutant proteins relative to that of Cys-less Hxt7 varied from 24 to 121% (Figure S1B of the Supporting Information). We measured the transport activity of the 21 single-Cys mutants over 5 s at 30 °C with 0.1 mM D-glucose as the substrate. Four single-Cys mutants (Y208C, Q209C, G215C, and I216C) manifested glucose transport activities of <10% of that of Cys-less Hxt7 (Figure 1A), which were too low for further study of pCMBS sensitivity. Given the wide range of expression levels for the mutant proteins, we also normalized transport activity to the expression level (Figure 1B). No substantial differences between the pattern of activities normalized by cell number and that of those normalized by expression level were apparent for these four low-activity mutants.

Characterization of Y208X and Q209X Mutants of Wild-Type Hxt7. Among the four sites sensitive to Cys replacement (Tyr^{208}, Gln^{209}, Gly^{215}, and Ile^{216}), only Tyr^{208} and Gln^{209} were potentially able to recognize the substrate either by $\pi-\pi$ interaction or by hydrogen bonding. We individually replaced Tyr^{208} and Gln^{209} of wild-type Hxt7 with each of the other 19 amino acids and measured the transport activities of the resulting proteins with D-glucose at a concentration of 0.1 or 20 mM (Figure 2). No substantial glucose transport activity was observed for any of the Q209X mutants with 0.1 mM D-glucose as the substrate (Figure 2B), whereas several Y208X mutants manifested such activity (Figure 2A). Among these functional Y208X mutants, both Y208F and Y208W exhibited transport activities similar to that of wild-type Hxt7, suggesting that the presence of an aromatic residue at site 208 is important

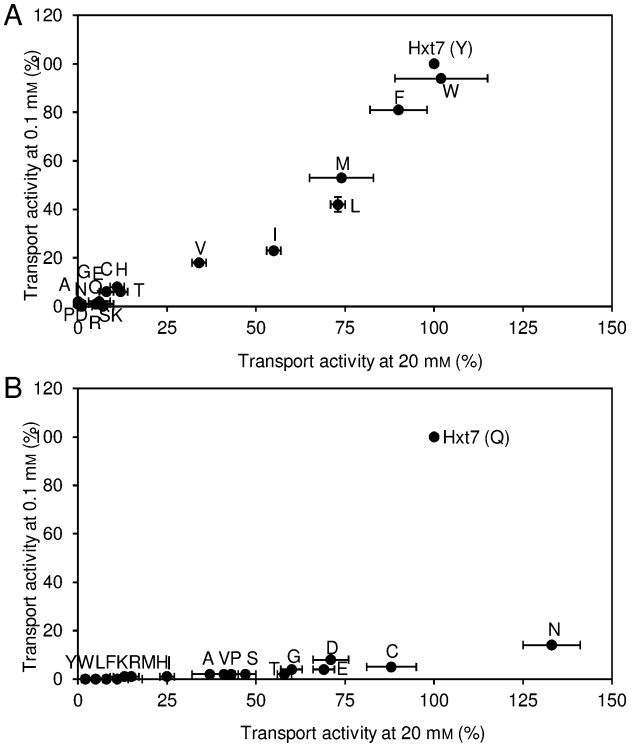

Figure 2. Glucose transport activities of the Y208X and Q209X series of mutants of wild-type Hxt7. KY73 cells expressing each of the Y208X (A) or Q209X (B) mutant proteins were grown to log phase at 30 °C in SMal(ura) medium, after which glucose transport activity was measured for 5 s at 30 °C with D-glucose at a concentration of 0.1 or 20 mM as the substrate. Transport activities were normalized by cell number and expressed as a percentage of the value for wild-type Hxt7. Data are means ± SE ($n \geq 3$).

for such activity. The expression level of the Y208X series of mutants varied from 19 to 97% relative to that of Hxt7 (Figure S2 of the Supporting Information), whereas that of the Q209X series of mutants was similar to that of the wild-type protein with the exception of those of Q209F (42%) and Q209H (35%) (Figure S3 of the Supporting Information). Several mutants of the Q209X series exhibited substantial transport activity with 20 mM D-glucose as the substrate (Figure 2B), suggesting that Gln^{209} is essential for high-affinity glucose transport by Hxt7.

Effects of pCMBS on Single-Cys Mutants of TM5. We examined the effects of pCMBS on the glucose transport activity of the 17 single-Cys mutants that retained a substantial level of activity (Figure 1C). In the presence of 0.5 mM pCMBS and with 0.1 mM D-glucose as the substrate, the glucose transport activity of Cys-less Hxt7 was inhibited by <10%. The transport activities of I212C, T213C, and N223C mutants were inhibited by >75% by pCMBS, whereas that of Y220C was increased by 79%. All of the sites sensitive either to Cys replacement or to pCMBS treatment are predicted to be clustered in one face of TM5 (Figure 3). We measured the IC_{50} values of pCMBS for the I212C, T213C, and N223C mutants (Figure 1D). The transport activities of I212C and N223C were not completely inhibited even in the presence of 0.5 mM pCMBS, whereas that of the T213C mutant was completely inhibited by this concentration of pCMBS, with the IC_{50} being 24 ± 2 μM [mean ± SE (n = 3)]. The pCMBS sensitivity of T213C was ~10 times that of wild-type Hxt7, for which the

dx.doi.org/10.1021/bi200958s | Biochemistry 2011, 50, 8674–8681

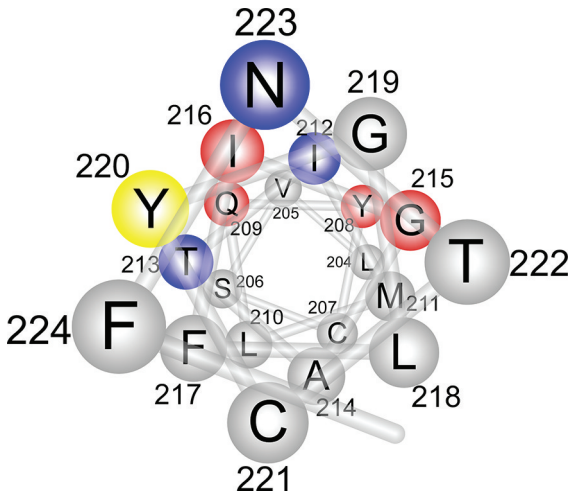

Figure 3. Helical-wheel representation of TM5 of Hxt7 shown from the extracellular side. Red circles represent residues for which Cys substitution resulted in mutants with low glucose transport activities (<10% of that of Cys-less Hxt7). Blue circles indicate residues for which single-Cys mutants were inhibited by pCMBS, and the yellow circle indicates a residue for which the single-Cys mutant was stimulated by pCMBS. All pCMBS-accessible sites and residues sensitive to Cys replacement are clustered in one face of TM5.

IC_{50} is ~250 μM.[12] The addition of 20 mM D-glucose or 2-deoxy-D-glucose, but not that of 20 mM L-glucose (a nontransportable sugar), significantly protected the T213C mutant from pCMBS inhibition (Table 1), indicating that Thr^{213} is located in the substrate translocation pathway.

Table 1. Protection of the T213C Mutant of Cys-less Hxt7 from pCMBS Inhibition by Substrate[a]

	without pCMBS		with pCMBS	
substrate added	D-glucose transport activity (pmol per 10^7 cells per 5 s)	%	D-glucose transport activity (pmol per 10^7 cells per 5 s)	%
none	9.8 ± 0.0	100	3.1 ± 0.1	32
D-glucose	9.9 ± 0.1	101	6.4 ± 0.2	65
2-deoxy-D-glucose	8.1 ± 0.2	83	6.1 ± 0.2	62
L-glucose	9.0 ± 0.2	92	3.0 ± 0.0	31

[a]KY73 cells expressing the single-Cys mutant T213C of Cys-less Hxt7 were grown to log phase at 30 °C in SMal(ura) medium and then washed three times with transport assay medium consisting of 50 mM MES-NaOH (pH 6.0) and 2 mM $MgSO_4$. Portions of the cell suspension were then incubated at room temperature first with or without the indicated substrate (20 mM) for 5 min and then in the additional absence or presence of 50 μM pCMBS for 15 min. The cells were then washed twice with 100 volumes of transport assay medium before measurement of glucose transport activity (3×10^7 to 5×10^7 cells) at 30 °C for 5 s with 0.1 mM D-[^{14}C]glucose as the substrate. Data are means ± SE (n = 3).

Characterization of T213X Mutants of Wild-Type Hxt7. To evaluate the role of Thr^{213} in glucose transport activity, we investigated the differences in the kinetics of glucose transport among the T213X series of mutants, in which Thr^{213} of wild-type Hxt7 is replaced with each of the other 19 amino acids. We first measured transport activities with D-glucose at a concentration of 0.1 or 20 mM (Table 2). T213F, T213W, T213P, and T213Q mutants were inactive. T213L, T213I, T213M, T213Y, T213E, T213H, T213K, and T213R

Table 2. Transport Activities of the T213X Series of Mutants of Wild-Type Hxt7 with Low (0.1 mM) and High (20 mM) Concentrations of D-Glucose as the Substrate[a]

	glucose transport in 0.1 mM D-glucose		glucose transport in 20 mM D-glucose	
	pmol per 10^7 cells per 5 s	normalized by IB	pmol per 10^7 cells per 5 s	normalized by IB
wild-type Hxt7(T)	89.0 ± 5.3	1.00	580 ± 46	1.00
T213G	7.2 ± 0.6	0.08	612 ± 13	1.04
T213A	13.1 ± 0.3	0.14	783 ± 36	1.27
T213V	32.7 ± 2.7	0.46	138 ± 18	0.30
T213L	0.2 ± 0.1	0.00	6 ± 34	0.02
T213I	0.2 ± 0.1	0.00	21 ± 25	0.05
T213F	0.2 ± 0.1	0.00	0 ± 4	0.00
T213W	0.0 ± 0.1	0.00	0 ± 2	0.00
T213M	0.1 ± 0.1	0.00	18 ± 37	0.04
T213C	29.5 ± 1.5	0.41	535 ± 31	1.10
T213P	0.0 ± 0.0	0.00	0 ± 3	0.00
T213S	19.8 ± 0.3	0.22	1133 ± 62	1.93
T213Y	0.0 ± 0.1	0.00	17 ± 37	0.03
T213N	4.1 ± 0.1	0.05	390 ± 21	0.61
T213Q	0.0 ± 0.1	0.00	0 ± 0	0.00
T213D	4.4 ± 0.2	0.06	372 ± 21	0.83
T213E	0.3 ± 0.1	0.00	36 ± 22	0.08
T213H	0.0 ± 0.1	0.00	48 ± 53	0.10
T213K	0.2 ± 0.2	0.00	6 ± 23	0.01
T213R	0.2 ± 0.1	0.00	26 ± 14	0.04

[a]The mutants were generated by replacement of Thr^{213} of wild-type Hxt7 with each of the other 19 amino acids. KY73 cells expressing each mutant protein were grown to log phase at 30 °C in SMal(ura) medium, and then glucose transport activity was measured for 5 s at 30 °C with 0.1 or 20 mM D-glucose as the substrate. Transport activities were normalized on the basis of cell number [data are means ± SE ($n \geq 3$)] or by the expression level of each mutant as determined by quantitative immunoblot (IB) analysis (Figure S4 of the Supporting Information) and then expressed relative to the value for wild-type Hxt7.

mutants had no activity with 0.1 mM D-glucose and low activity (<10% of that of wild-type Hxt7) with 20 mM D-glucose. Only seven T213X mutants were functional transporters, although no substantial differences in expression level were observed among the T213X series of mutants (Figure S4 of the Supporting Information); the extent of expression of each mutant protein was thus 61−109% of that of wild-type Hxt7, with the exception of that of T213L (49%). The K_m, V_{max}, and transport efficiency (V_{max}/K_m) values for the seven functional T213X mutants were determined under the zero-trans entry condition with 0.1−60 mM D-glucose as the substrate (Table 3). These mutants exhibited a wide range of K_m values, from 0.40 to 34 mM, whereas V_{max} values normalized by expression level varied slightly from 0.8 to 2.2 relative to that of Hxt7 with the exception of that of T213V (0.3). Replacement of Thr^{213} with Val yielded a glucose transporter with an affinity for glucose (K_m = 0.40 ± 0.02 mM) that was higher than that of wild-type Hxt7 (K_m = 0.72 ± 0.07 mM); this replacement did not result in a high transport efficiency (V_{max}/K_m), however, with the value being only half that of Hxt7 after normalization by expression level.

We previously demonstrated that the size of amino acid residues is an important determinant of high affinity for glucose. Replacement of Asp^{340} in TM7 of Hxt7 with Cys, Ala,

dx.doi.org/10.1021/bi200958s | Biochemistry 2011, 50, 8674−8681

Table 3. Kinetic Parameters of T213X Mutants of Wild-Type Hxt7[a]

		V_{max}		V_{max}/K_m	
	K_m (mM)	pmol per 10^7 cells per 5 s	normalized by IB	pmol per 10^7 cells per 5 s per mM	normalized by IB
wild-type Hxt7(T)	0.72 ± 0.07	560 ± 30	1.00	760 ± 30	1.00
T213G	22 ± 6	1020 ± 210	1.80	46 ± 2	0.06
T213A	16 ± 4	1290 ± 320	2.17	82 ± 2	0.10
T213V	0.40 ± 0.02	120 ± 0	0.27	310 ± 20	0.51
T213C	1.6 ± 0.1	380 ± 30	0.81	230 ± 10	0.36
T213S	6.6 ± 0.5	910 ± 140	1.61	140 ± 10	0.18
T213N	34 ± 4	960 ± 50	1.57	29 ± 2	0.04
T213D	13 ± 1	330 ± 20	0.77	26 ± 2	0.04

[a]KY73 cells expressing each mutant were grown to log phase at 30 °C in SMal(ura) medium, after which glucose transport activity was measured for 5 s at 30 °C with 0.1−60 mM D-glucose as the substrate. Transport activities were normalized by cell number (data are means ± SE from at least three independent experiments), or they were normalized by the expression level of each mutant as determined by quantitative immunoblot (IB) analysis (Figure S4 of the Supporting Information) and then expressed relative to the value for wild-type Hxt7. The transport activities of the T213L, T213I, T213F, T213W, T213M, T213P, T213Y, T213Q, T213E, T213H, T213K, and T213R mutants were too low for the determination of kinetic parameters.

Ile, and Val thus generated high-affinity glucose transporters.[12] Similar effects of residue replacement at Asn^{331} of Hxt2 [11] and at Ile^{287} of human GLUT1,[19] each corresponding to Asp^{340} of Hxt7, were observed with Val, Ile, and Cys in Hxt2 and with Val in GLUT1, suggesting the existence of a common structure around this position in both yeast and mammalian high-affinity glucose transporters. We analyzed data from the crystal structures of the MFS transporters LacY,[5] GlpT,[6] and EmrD[7] and calculated the average side chain length of each residue (Table 4). There was no marked difference in side chain length for a given residue between all regions and TM regions of these transporters. The side chain length of the mutant residues in the T213X mutant proteins with high-affinity glucose transport activity (T213V and T213C) and with moderately high-affinity glucose transport activity (T213S) was limited to ∼2.5 Å (Figure 4). In addition, the mutant residues of all the functional T213X mutants possessed a side chain length of <3.6 Å. The T213P mutant is the only nonfunctional member of the T213X series for which the side chain length of the mutant residue was <3.6 Å. Our results of cysteine-scanning analysis of TM5 and the effects of pCMBS indicated that Thr^{213} is located at or close to a substrate binding site, but it does not appear to contribute to a strong direct interaction with the substrate, given that a common feature of residues conferring glucose transport activity at this position is the possession of a side chain length of <3.6 Å.

We next examined the substrate specificities of mutants T213V and T213C and Hxt7. No substantial differences in the effects of the addition of nonradioactive sugars on D-[^{14}C]glucose transport were observed between the mutants and wild-type Hxt7, with the exception of the activities

Table 4. Distances[a] between the α-Carbon and the Most Distant Atom Except Hydrogen in the Side Chain for the α-Carbon for Each Type of Amino Acid Residue in LacY,[5] GlpT,[6] and EmrD[7]

	TM regions		all regions	
amino acid	n	average ± SD (Å)	n	average ± SD (Å)
Ala	83	1.517 ± 0.018	118	1.520 ± 0.024
Arg	12	6.781 ± 0.790	44	6.830 ± 0.825
Asn	16	3.550 ± 0.226	36	3.584 ± 0.190
Asp	10	3.569 ± 0.224	25	3.556 ± 0.187
Cys	18	2.815 ± 0.061	21	2.817 ± 0.070
Gln	15	4.488 ± 0.539	30	4.581 ± 0.711
Glu	7	4.602 ± 0.464	27	4.588 ± 0.699
Gly	94	0 ± 0	123	0 ± 0
His	2	4.630 ± 0	12	4.587 ± 0.079
Ile	62	3.669 ± 0.541	81	3.675 ± 0.567
Leu	121	3.773 ± 0.384	169	3.799 ± 0.358
Lys	7	5.941 ± 0.484	29	5.919 ± 0.908
Met	46	4.531 ± 0.923	59	4.541 ± 0.916
Phe	85	5.099 ± 0.088	108	5.097 ± 0.087
Pro	31	2.407 ± 0.014	55	2.410 ± 0.023
Ser	40	2.429 ± 0.036	71	2.429 ± 0.044
Thr	32	2.514 ± 0.032	56	2.518 ± 0.038
Trp	17	6.119 ± 0.624	30	6.188 ± 0.645
Tyr	31	6.449 ± 0.127	42	6.450 ± 0.146
Val	69	2.522 ± 0.044	90	2.524 ± 0.046

[a]The distance was calculated and averaged for each type of amino acid among the residues located in TM regions or in all regions.

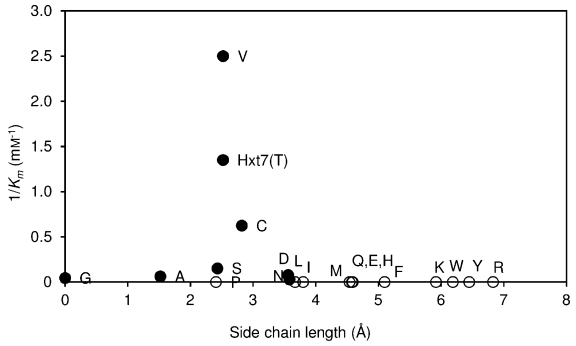

Figure 4. Affinities of the T213X series of mutants of wild-type Hxt7 for D-glucose vs the side chain length of the mutant residue. KY73 cells expressing the indicated T213X mutants of wild-type Hxt7 were cultured to log phase at 30 °C in SMal(ura) medium, after which the kinetic parameters of D-glucose transport were measured for 5 s at 30 °C with D-glucose at concentrations of 0.1−60 mM. Affinity is expressed as $1/K_m$, with values being means from at least three independent experiments. Each circle represents a value for an individual mutant according to the indicated code, with filled circles denoting mutants for which kinetic analysis was performed (Table 3). The side chain length of each amino acid was obtained from the residues located in all regions in the crystal structures of LacY,[5] GlpT,[6] and EmrD[7] as shown in Table 4.

dx.doi.org/10.1021/bi200958s | Biochemistry 2011, 50, 8674−8681

measured in the presence of 6-deoxy-D-glucose (Figure 5). We measured the inhibition constant (K_i) for 6-deoxy-D-glucose

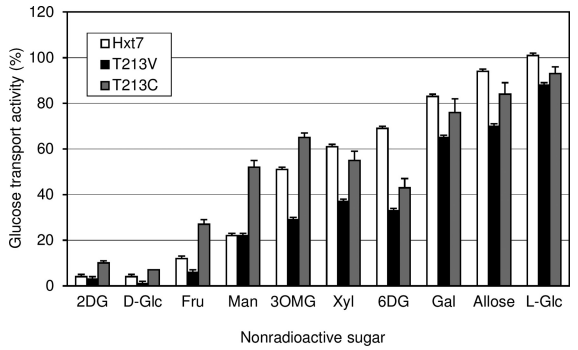

Figure 5. Substrate specificity of wild-type Hxt7 and its T213V and T213C mutants. Transport activities were measured at 30 °C for 5 s with 0.1 mM D-[^{14}C]glucose as the substrate in the presence of the indicated nonradioactive sugars at 20 mM. The glucose transport activity of each protein was expressed as a percentage of that determined in the presence of 20 mM sorbitol. Data are means ± SE ($n \geq 4$). Abbreviations: 2DG, 2-deoxy-D-glucose; D-Glc, D-glucose; Fru, D-fructose; Man, D-mannose; 3OMG, 3-*O*-methyl-D-glucose; Xyl, D-xylose; 6DG, 6-deoxy-D-glucose; Gal, D-galactose; Allose, D-allose; L-Glc, L-glucose.

with 0.05 mM D-[^{14}C]glucose as the substrate, obtaining a value of 38 ± 6 mM for Hxt7 compared with values of 12 ± 2 mM for the T213V mutant and 13 ± 2 mM for the T213C mutant [means ± SE ($n \geq 3$)]. These low K_i values for the mutants suggested that recognition of the C6 position of glucose was slightly affected in the mutant proteins. We also examined the role of Tyr^{220} (given that the transport activity of the single-Cys Y220C mutant was stimulated by pCMBS) by replacing this residue of Hxt7 with the other aromatic residues (Phe or Trp) or with the nonaromatic residues Cys, Ile, and Met (data not shown). The K_m values for all these mutants were ~1 mM, with the exception of that for Y220W (7.2 mM), indicating that Tyr^{220} is neither a key residue in determination of substrate affinity nor an essential aromatic residue.

Location of Important Residues Inferred from a Homology Model of Hxt7. To speculate about the functional roles of the identified residues of Hxt7, we constructed a homology model of Hxt7 based on the crystal structure of GlpT. The alignment of GlpT and Hxt7 adopted is shown in Figure 6, which we obtained from our previous alignment[10] with a slight modification. As shown in Figure 6, there was very poor sequence similarity between GlpT and Hxt7, so we built the sequence alignment by referencing structural features suggested by several structure prediction tools described in Experimental Procedures. Although we could not claim that the proposed structure of Hxt7 is sufficiently trustworthy, the proposed structural model was quite reasonable for speculating about the structure–function relationship revealed by our experimental data, as discussed below. In Figure 7, Thr^{213} is located deep within the membrane and facing the central substrate pathway. One helix turn below Thr^{213}, Gln^{209} faces the central pathway, and the amide group in the side chain of Gln^{209} is implicated as a coordinating group for glucose. The environment surrounding Gln^{209} appears to be critical for tuning the structure of a high-affinity glucose transporter. Asp^{340} in TM7, a residue that we previously identified as a key residue for high-affinity glucose transport by Hxt7,[12] is within

```
TM5:
Hxt7    199 HLRGTLVSCYQLMITAGIFLGYC 221
Hxt2    190 HIRGTCVSFYQLMITLGIFLGYC 212
GLUT1   151 ALRGALGTLHQLGIVVGILIAQV 173
GlpT    155 GGIVSVWNCAHNVGGGIPPLLFL 177
                    *   *
TM7:
Hxt7    322 LQRLIMGAMIQSLQQLTGDNYFFYYG 347
Hxt2    313 LPRVIMGIMIQSLQQLTGNNYFFYYG 338
GLUT1   269 RQPILIAVVLQLSQQLSGINAVFYYS 294
GlpT    255 LWYIAIANVFVYLLRYGILDWSPTYL 280
                              *
```

Figure 6. Alignments of TM5 and TM7 adopted for the homology model. Alignment of the TMs of Hxt2 (*S. cerevisiae*), Hxt7 (*S. cerevisiae*), GLUT1 (*Homo sapiens*), and GlpT (*E. coli*) was performed with ClustalW and then modified manually. Each of the TM segments was enclosed with a box. Amino acid residues important for high-affinity glucose transport activity of Hxt7 shown in Figure 7 are denoted with asterisks.

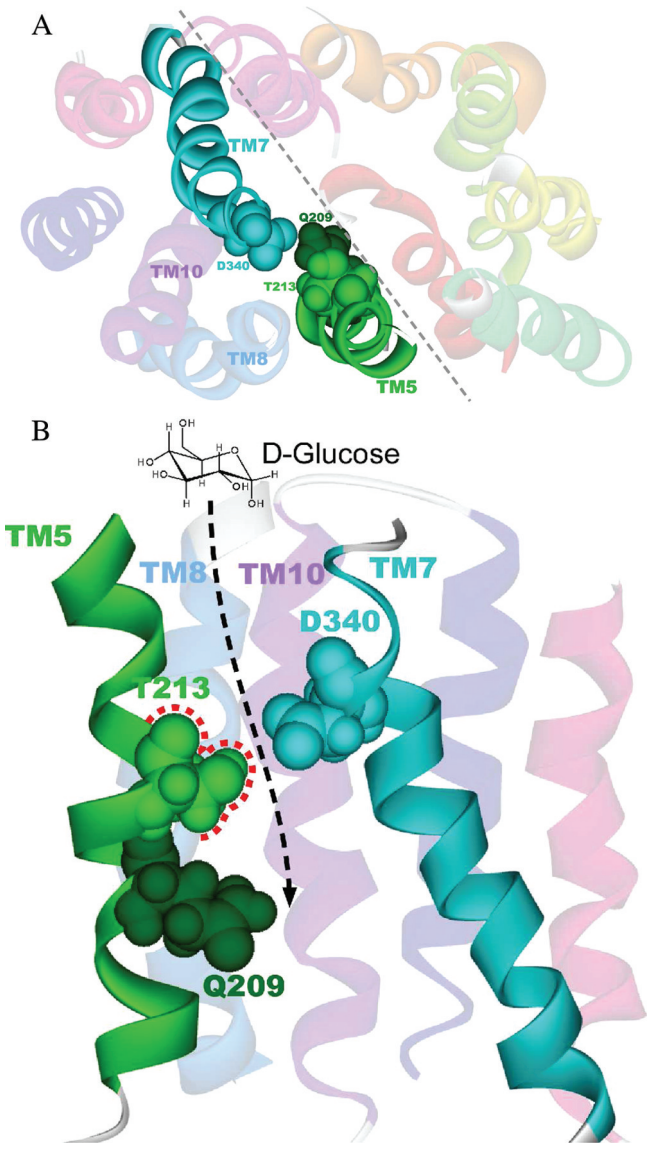

Figure 7. Hypothetical 3D core structure of Hxt7. The structure was generated with the protein modeling tool MODELER and with GlpT as a reference structure and sequence alignment based on sequence similarity (Figure 6): (A) top view from the extracellular side (broken line, cutting line for the side view) and (B) side view.

dx.doi.org/10.1021/bi200958s | *Biochemistry* 2011, 50, 8674–8681

van der Waals distance of Thr^{213} (Figure 7). Replacement of Thr^{213} with residues of similar size such as Val, Cys, and Ser did not appear to affect the interaction between residue 213 and Asp^{340}, and the corresponding mutants retained high-affinity transport activity. Replacement of Thr^{213} with smaller residues such as Gly and Ala resulted in an increase in the distance between residue 213 and Asp^{340}, and a weakened van der Waals force disturbed the structure of the high-affinity glucose transporter. Replacement of Thr^{213} with bulky residues resulted in steric hindrance, and a loss of van der Waals interaction resulted in a loss of glucose transport activity. It is noted that not only Thr^{213} (TM5) and Asp^{340} (TM7) but also other residues in TM8 and TM10 seem to contribute to determine the form of the substrate pathway (Figure 7).

Comparison with Other Transporters. Our observation that pCMBS-sensitive sites cluster to form one face of a hydrophilic region in TM5 of Hxt7 provides experimental evidence that supports the notion that TM5 contributes to the substrate translocation pathway. A previous analysis of all 12 TMs of human GLUT1 by cysteine mutagenesis in conjunction with pCMBS treatment found that pCMBS-sensitive sites in TM5 clustered to form one face of hydrophilic residues,[20,21] consistent with our observations with Hxt7 described here. Mutation of Val^{197} to Ile in human GLUT2, which corresponds to Thr^{213} in Hxt7, a residue we have now shown to be an important determinant of substrate affinity, was detected in a diabetic patient and was confirmed to give rise to a nonfunctional transporter in a heterologous expression system,[22] suggesting that the size of the amino acid at this position is also important in GLUT2. All members of the Hxt family possess Thr at this site, suggesting that Thr^{213} of Hxt7 is not the sole residue determining substrate affinity. Glutamine 161 in GLUT1, which corresponds to Gln^{209} in Hxt7, was also previously shown to be critical for transport activity, given that both Q161V and Q161N mutants of GLUT1 manifested reduced activity relative to that of the wild-type protein.[23] We showed that the equivalent residue is essential in Hxt7 by generating a series of Q209X mutants and finding that no other residue was able to substitute for Gln^{209}. Glutamine at this position is also conserved among all members of the Hxt family[1] as well as in most members of the GLUT family with the exception of GLUT9 (Ala), GLUT11 (Ala), and HMIT (Thr).[24] A common mechanism of substrate recognition around TM5 thus seems to operate in both yeast hexose transporters and mammalian glucose transporters, although the level of amino acid sequence identity between Hxt7 and GLUT1 is <30% even within TM regions.[25] Cysteine-scanning mutagenesis of TM5 in OxlT of *O. formigenes* also revealed that TM5 contributes to the substrate pathway on the basis of the observation that several sites within this TM were sensitive to thiol-directed methanethiosulfonate-linked agents and that they were protected from such agents by the addition of substrate.[26] In addition, a Pro residue in the center of TM5 in OxlT appeared to introduce a kink into the α-helix, and the methanethiosulfonate-sensitive sites were not clustered in one face. Hxt7 does not contain Pro in TM5, suggesting structural differences around TM5 between the two transporters.

We found that only small amino acids were able to support glucose transport activity at residue 213 of Hxt7. Small side chains are important for stabilization of helical membrane proteins and allow conformational changes in the protein structure because associations between α-helices are governed by electrostatic and van der Waals interactions,[27] consistent with our results showing the importance of side chain length for substrate affinity in a glucose transporter. For human glucose transporters of the GLUT (SLC2A) family, Manolescu et al. proposed possible hydrophobic interactions during the transport process, and they postulated that the side chain length of hydrophobic residues that line but are located at the ends of the substrate pathway influences substrate selectivity through hydrophobic interactions with the water shell surrounding the substrate on the basis of a fructose-docking homology model of GLUT7.[28] Our results show that the size of the residues at positions 213 (this study) and 340[12] is crucial for the high-affinity glucose transport activity of Hxt7 but not for substrate specificity. Both of these sites are located not at the ends but in the middle of TMs, which may explain differences with GLUT proteins in the effects of hydrophobic interactions. In this study of Hxt7, hydrophobic interactions among residues in TM5 and TM7, which constitute part of the central pore (Figure 7), may thus play a pivotal role in formation of a core structure that determines substrate affinity. In addition to the importance of side chain length, side chain shape should not be ignored as a determinant of the fine-tuning of transporter structure. Further study of other TMs that form the wall of the substrate translocation pathway is required to elucidate the molecular mechanism underlying the affinity of a transporter for glucose.

CONCLUSION

With the use of cysteine-scanning mutagenesis and by examination of the accessibility of substituted cysteine residues in TM5 of Hxt7 to the hydrophilic sulfhydryl reagent pCMBS, we have revealed that the sites sensitive either to Cys replacement or to pCMBS cluster to form one face of this TM. Among the sites sensitive to Cys replacement, Gln^{209} was found to be an essential residue for high-affinity glucose transport activity, whereas among sites insensitive to Cys replacement, Thr^{213} was found to be located at or close to a substrate recognition site. Furthermore, we examined the role of Thr^{213} by replacing it with each of the other 19 amino acids and found that it is a key residue for determination of substrate affinity. The side chain length of the residue at position 213 was thus a critical determinant of high-affinity glucose transport activity. In our working homology model of Hxt7, Thr^{213} (TM5) and Asp^{340} (TM7) are positioned within van der Waals distance of each other and contribute to the substrate pathway. In the proximity of this interaction, the essential residue Gln^{209} faces the substrate translocation pathway, suggesting the importance of van der Waals interaction close to the substrate binding site for tuning of the structure of this high-affinity glucose transporter.

ASSOCIATED CONTENT

Supporting Information

Expression of 21 single mutants of TM5 (Figure S1), Y208X mutants (Figure S2), Q209X mutants (Figure S3), and T213X mutants (Figure S4). This material is available free of charge via the Internet at http://pubs.acs.org.

AUTHOR INFORMATION

Corresponding Author

*Telephone: +81-426-78-3261. Fax: +81-426-78-3262. E-mail: toshiko@main.teikyo-u.ac.jp.

Funding

This work was supported by grants from Teikyo University.

■ ACKNOWLEDGMENTS

We thank Dr. A. L. Kruckeberg (University of Montana - Missoula, Bozeman, MT) for yeast strain KY73 as well as Dr. H. Kanazawa and Dr. A. Yamaguchi (Osaka University, Osaka, Japan) for helpful discussion.

■ ABBREVIATIONS

MFS, major facilitator superfamily; TM, transmembrane segment; 3D, three-dimensional; SD, standard deviation; SE, standard error; pCMBS, *p*-chloromercuribenzenesulfonate.

■ REFERENCES

(1) Kruckeberg, A. L. (1996) The hexose transpoter family of *Saccharomyces cerevisiae*. *Arch. Microbiol. 166*, 283−292.
(2) Boles, E., and Hollenberg, C. P. (1997) The molecular genetics of hexose transport in yeasts. *FEMS Microbiol. Rev. 21*, 85−111.
(3) Saier, M. H. Jr., Tran, C. V., and Barabote, R. D. (2006) TCDB: The transporter classification database for membrane transport protein analyses and information. *Nucleic Acids Res. 34*, D181−D186.
(4) Hirai, T., Heymann, J. A., Maloney, P. C., and Subramaniam, S. (2003) Structural model for 12-helix transporters belonging to the major facilitator superfamily. *J. Bacteriol. 185*, 1712−1718.
(5) Abramson, J., Smirnova, I., Kasho, V., Verner, G., Kaback, H. R., and Iwata, S. (2003) Structure and mechanism of the lactose permease of *Escherichia coli*. *Science 301*, 610−615.
(6) Huang, Y., Lemieux, M. J., Song, J., Auer, M., and Wang, D. N. (2003) Structure and mechanism of the glycerol-3-phosphate transporter from *Escherichia coli*. *Science 301*, 616−620.
(7) Yin, Y., He, X., Szewczyk, P., Nguyen, T., and Chang, G. (2006) Structure of the multidrug transporter EmrD from *Escherichia coli*. *Science 312*, 741−744.
(8) Dang, S., Sun, L., Huang, Y., Lu, F., Liu, Y., Gong, H., Wang, J., and Yan, N. (2010) Structure of a fucose transporter in an outward-open conformation. *Nature 467*, 734−738.
(9) Kasahara, T., and Kasahara, M. (2003) Transmembrane segments of 1, 5, 7 and 8 are required for high-affinity glucose transport by *Saccharomyces cerevisiae* Hxt2 transporter. *Biochem. J. 372*, 247−252.
(10) Kasahara, T., Ishiguro, M., and Kasahara, M. (2006) Eight amino acid residues in transmembrane segments of yeast glucose transporter Hxt2 are required for high affinity transport. *J. Biol. Chem. 281*, 18532−18538.
(11) Kasahara, T., Maeda, M., Ishiguro, M., and Kasahara, M. (2007) Identification by comprehensive chimeric analysis of a key residue responsible for high affinity glucose transport by yeast HXT2. *J. Biol. Chem. 282*, 13146−13150.
(12) Kasahara, T, and Kasahara, M. (2010) Identification of a key residue determining substrate affinity in the yeast glucose transporter Hxt7: A two-dimensional comprehensive study. *J. Biol. Chem. 285*, 26263−26268.
(13) Ye, L., Kruckeberg, A. L., Berden, J. A., and van Dam, K. (1999) Growth and glucose repression are controlled by glucose transport in *Saccharomyces cerevisiae* cells containing only one glucose transporter. *J. Bacteriol. 181*, 4673−4675.
(14) Kasahara, T., Ishiguro, M., and Kasahara, M. (2004) Comprehensive chimeric analysis of amino acid residues critical for high affinity glucose transport by Hxt2 of *Saccharomyces cerevisiae*. *J. Biol. Chem. 279*, 30274−30278.
(15) Amberg, D. C., Burke, D. J., and Strathern, J. N. (2005) Supplemented minimal medium (SMM). *Methods in Yeast Genetics*, pp 200−201, Cold Spring Harbor Laboratory Press, Plainview, NY.
(16) Nishizawa, K., Shimoda, E., and Kasahara, M. (1995) Substrate recognition domain of the Gal2 galactose transporter in yeast *Saccharomyces cerevisiae* as revealed by chimeric galactose-glucose transporters. *J. Biol. Chem. 270*, 2423−2426.
(17) Kasahara, M., Shimoda, E., and Maeda, M. (1997) Amino acid residues responsible for galactose recognition in yeast Gal2 transporter. *J. Biol. Chem. 272*, 16721−16724.
(18) Kasahara, T., and Kasahara, M. (1996) Expression of the rat GLUT1 glucose transporter in the yeast *Saccharomyces cerevisiae*. *Biochem. J. 315*, 177−182.
(19) Kasahara, T., Maeda, M., Boles, E., and Kasahara, M. (2009) Identification of a key residue determining substrate affinity in the human glucose transporter GLUT1. *Biochim. Biophys. Acta 1788*, 1051−1055.
(20) Mueckler, M., and Makepeace, C. (2009) Model of the exofacial substrate-binding site and helical folding of the human Glut1 glucose transporter based on scanning mutagenesis. *Biochemistry 48*, 5934−5942.
(21) Mueckler, M., and Makepeace, C. (1999) Transmembrane segment 5 of the Glut1 glucose transporter is an amphipathic helix that forms part of the sugar permeation pathway. *J. Biol. Chem. 274*, 10923−10926.
(22) Mueckler, M., Kruse, M., Strube, M., Riggs, A. W., Chiu, K. C., and Permutt, M. A. (1994) A mutation in the Glut2 glucose transporter gene of a diabetic patient abolishes transport activity. *J. Biol. Chem. 269*, 17765−17767.
(23) Mueckler, M., Weng, W., and Kruse, M. (1994) Glutamine 161 of Glut1 glucose transporter is critical for transport activity and exofacial ligand binding. *J. Biol. Chem. 269*, 20533−20538.
(24) Zhao, F.-Q., and Keating, A. F. (2007) Functional properties and genomics of glucose transporters. *Curr. Genomics 8*, 113−128.
(25) Baldwin, S. A. (1993) Mammalian passive glucose transporters: Members of an ubiquitous family of active and passive transport proteins. *Biochim. Biophys. Acta 1154*, 17−49.
(26) Wang, X., Ye, L., McKinney, C. C., Feng, M., and Maloney, P. C. (2008) Cysteine scanning mutagenesis of TM5 reveals conformational changes in OxlT, the oxalate transporter of *Oxalobacter formigenes*. *Biochemistry 47*, 5709−5717.
(27) Curran, A. R., and Engelman, D. M. (2003) Sequence motifs, polar interactions and conformational changes in helical membrane proteins. *Curr. Opin. Struct. Biol. 13*, 412−417.
(28) Manolescu, A. R., Witkowska, K., Kinnaird, A., Cessford, T., and Cheeseman, C. (2007) Facilitated hexose transporters: New perspectives on form and function. *Physiology 22*, 234−240.